Robotics and Autonomous Systems 113 (2019) 56–62

Contents lists available at ScienceDirect

Robotics and Autonomous Systems

journal homepage: www.elsevier.com/locate/robot

Testing of a torque vectoring controller for a Formula Student prototype

João Antunes [b], André Antunes [b], Pedro Outeiro [a,b,*], Carlos Cardeira [a,b], Paulo Oliveira [a,b]

[a] IDMEC, Universidade de Lisboa, Avenida Rovisco Pais, 1049-001 Lisboa, Portugal
[b] Instituto Superior Técnico, Universidade de Lisboa, Avenida Rovisco Pais, 1049-001 Lisboa, Portugal

HIGHLIGHTS

- Torque vectoring control was achieved using low-cost sensors.
- Testing was performed on a Formula Student race car.
- The Burckhardt Tire Model was used providing easier implementation on other vehicles.

ARTICLE INFO

Article history:
Available online 2 January 2019

Keywords:
Torque control
Control systems
Optimal control
System implementation

ABSTRACT

The torque vectoring controller is the electrical substitute of a mechanical differential, with the advantage of improving the stability and handling of the vehicle. This work tackles the design, implementation and testing of a torque vectoring algorithm to be implemented in a Formula Student prototype. First is presented a dynamic test model used for the design and tuning of the controllers, which is then validated with real data from a real vehicle. Secondly, a computation methodology to achieve a reference value is proposed. Two controllers are presented, a PID and a LQR controller, with both being designed and tested in simulation. In a final part, the two controllers are implemented in a Formula Student prototype. The results from the vehicle with and without the controllers are then compared and the performance improvement discussed.

1. Introduction

Every year, automotive companies implement new and better control algorithms in public commercial vehicles. These are used to increase the safety of the vehicle occupants and those surrounding it, to increase the performance, and even to enhance the driving experience. Examples of these widespread algorithms are the Anti-Lock Braking System (ABS), the Electronic Stability Program (ESP) and the Traction Control (TC). More recently, to evolve to autonomous driving, algorithms that aid the driver in the driving task are also starting to appear like the Lane Assist, and the City Emergency Brake.

This work tackles another type of vehicle stability control, the Torque Vectoring (TV). The TV is based on the concept of redistributing the torque in each wheel to help the vehicle turn more efficiently. This algorithm considers the more direct approach where the vehicle is equipped with independent electric motors. All the development of this work is focused on a Formula Student vehicle implementation.

Formula Student is a worldwide inter-university competition for students, where each team develops, constructs, and races a single-seat formula style racing vehicle. With the objective of building a better and more advanced vehicle, and driven by the organization, the competition has been evolving from year to year. The IST team has participated in several of these competitions and had an interest in exploring more recent assisted driving control methods, hence the interest in studying the use of TV for their cars. By participating in the Formula Student team, it was possible to learn about the inner workings of cars, electronics, aerodynamics, how to manage and work in large projects. It also provides an opportunity to gain contacts with companies, as a major part of the project is finding sponsors willing to provide components for the prototype.

The torque vectoring system can be tackled using several approaches. The most common is using the yaw rate of the vehicle as in [1,2]. In [1] it is proposed the use of a control logic for left right torque vectoring which allows maximization of the extractable lateral force from the tires by making them work in the optimal operating region, while [2] uses a Linear Parameter-Varying (LPV)

* Correspondence to:Universidade de Lisboa, Avenida Rovisco Pais, 1049-001 Lisboa, Portugal.
E-mail addresses: joao.pedro.antunes@tecnico.ulisboa.pt (J. Antunes), andre.antunes@tecnico.ulisboa.pt (A. Antunes), pedro.outeiro@tecnico.ulisboa.pt (P. Outeiro), carlos.cardeira@tecnico.ulisboa.pt (C. Cardeira), paulo.j.oliveira@tecnico.ulisboa.pt (P. Oliveira).

https://doi.org/10.1016/j.robot.2018.12.010
0921-8890/

gain-scheduled controller for tracking the longitudinal velocity and the yaw rate of the vehicle and a linearly interpolated Torque and Slip Limiter (TSL) for coping with saturation of the electric motors and wheel slip limitations. More complex algorithms also use the sideslip angle observation like [3–5]. In [3] a LQG controller, a flat feed forward controller, and a linear desired value generator are proposed for influencing lateral vehicle dynamics, while [4] compares two second-order sliding-mode controllers against a feedforward controller combined with either a conventional or an adaptive PID controller, and [5] proposes a new Sliding mode controller using a nonlinear 2 DOF vehicle model and a sliding surface that integrates the vehicle yaw-rate error and slip angle error. Several designs can be implemented, but the most basic, and still reliable, method is the distribution of the torque between the left and right wheels proportional to the steering angle. The use of PID control is also considered in [6], where PID and LP methods are considered for the implementation of Torque vectoring in a hydrogen powered racing vehicle. The use of PID, as proposed in [4,6], provides a simple method to implement and tune, which is advantageous. In [4,5] sliding mode control is used in order to track the yaw rate and slip angle. Some other authors make use of predictive control to find the optimal control inputs like [7,8]. In [7] a vehicle yaw stability control system based on the generalized predictive control (GPC) method is proposed, while [8] proposes the use of a model predictive control (MPC) strategy. Additionally, some authors use Fuzzy control to make the torque allocation per wheel, like in [9] where a fuzzy logic controller is developed to explore the feasibility and capability of BBW systems for lateral control and yaw stability control.

In this paper, a solution using low cost sensors and off the shelf embedded systems is proposed. The use of PID and LQR solutions is considered. Additionally, the proposed solution was studied with implementation in real time and with validation and testing in a real vehicle.

In this work, first the main equations for a vehicle model are presented, used for testing and calibrating the algorithm. This model is validated using real data from a Formula Student vehicle. Then, two different controllers, namely a PID and a LQR controller, are studied, and a method to compute the reference is advanced. Both algorithms are implemented and tested in a Formula Student vehicle. Finally, the performance of the controllers is assessed in the vehicle.

2. Vehicle model

In order to design, evaluate and tune the controllers is proposed a vehicle model. In this section are presented the adopted model and assumptions used for each part. Simulation models can be very complex with several degrees of freedom or can be a simple 2 degree of freedom model [10, p. 6]. For this work a complex version, depicted in Fig. 1, is used for testing relying on the non-linear equations presented ahead. For the controllers a widely used linearized version [11–13] is adopted, with a small modification required for the controller.

The model is based on the FST06e, the vehicle for which the controllers are being studied. This platform, is a full electric Formula Student car, powered by two independent permanent magnet synchronous motors (PMSM) from Siemens. Each motor has 50 kW, the torque is amplified by a 4.4:1 fixed planetary gear, resulting in a total of 877 N m at the rear wheels.

2.1. Non-linear model

The core of the non-linear vehicle model is the planar movement given by (1)–(3), respectively dictating the dynamics of the forward (v_x) and lateral (v_y) velocities, and of the heading of the car (ψ). Where each tire is presumed to generate a longitudinal (F_x) and a lateral (F_y) force in the wheel frame $\{w\}$, and the front (F) and rear (R) tires are positioned at a distance of l_f and l_r, respectively, from the center of gravity of the car. There is an aerodynamic drag force (F_{drag}) acting upon the car. The steering angle of the front wheels is represented by δ. The mass is represented by m, the inertia by I_{zz}. This is a balance of the forces acting on the vehicle by the tires, with only a simple modification implemented, namely the introduction of the torque (M_z) generated by different forces generated by the driven wheels. This will be the actuation of the torque vectoring controller.

$$\dot{v}_x = v_y\dot{\psi} - \frac{1}{m}\left[F_y^F \sin\delta - F_x^F \cos\delta - F_x^R\right] - F_{drag} \tag{1}$$

$$\dot{v}_y = -v_x\dot{\psi} + \frac{1}{m}\left[F_y^F \cos\delta + F_y^R + F_x^F \sin\delta\right] \tag{2}$$

$$\ddot{\psi} = \frac{1}{I_{zz}} l_f \left[F_y^F \cos\delta + F_x^F \sin\delta\right] - \frac{1}{I_{zz}} l_r F_y^R + \frac{M_z}{I_{zz}} \tag{3}$$

$$\mu_r(s_r) = C_1\left(1 - e^{-C_2 s_r}\right) - C_3 s_r \quad , \quad s_r = \sqrt{s_s^2 + s_l^2} \tag{4}$$

For the computation of the forces generated by the tires, a simplified version of the Burckhardt Tire Model [14] for the friction coefficient (μ_r), given by (4), is used. The slip factors s_s and s_l are given in Table 1, where i is the wheel index, v_i^c is the velocity of the vehicle, v_i^w is the linear equivalent velocity of the wheel, α_i is the slip angle of the wheel given by (5), and (x_i, y_i) is the wheel position.

$$\alpha_i = \mathrm{tg}^{-1}\left(\frac{v_y + x_i\dot{\psi}}{v_x - y_i\dot{\psi}}\right) - \delta \tag{5}$$

The C_1, C_2 and C_3 constants parameterize the tire model for different tire-road conditions. The vertical load in each wheel is given by a steady state load transfer to an acceleration input [12].

Table 1
Longitudinal and lateral slip equations for driving and braking conditions.

Longitudinal slip		Lateral slip	
Braking	Driving	Braking	Driving
$s_l^i = \frac{v_i^w \cos\alpha_i - v_i^c}{v_i^c}$	$s_l^i = \frac{v_i^w \cos\alpha_i - v_i^c}{v_i^w \cos\alpha_i}$	$s_s^i = \frac{v_i^w \sin\alpha_i - v_i^c}{v_i^c}$	$s_s^i = \mathrm{tg}^{-1}(\alpha_i)$

2.2. Linear model

The linear model used is the standard bicycle model, a common approximation found in literature [12,15]. The linearization of Eqs. (1)–(3) for a small angle and a constant longitudinal velocity, results in (6), where the steering angle δ is considered a disturbance by the driver, and M_z the input to be actuated by the controller. For this model, it is also assumed the cornering stiffness approximation ($F_y = C_y\alpha$) for the lateral forces instead of a tire model.

The variables of FST06e to simulate both models are presented in Table 2.

$$\begin{bmatrix}\dot{v}_y \\ \ddot{\psi}\end{bmatrix} = \begin{bmatrix} -\frac{C_{y,f} + C_{y,r}}{m v_x} & \frac{-l_f C_{y,f} + l_r C_{y,r}}{m v_x} - v_x \\ \frac{-l_f C_{y,f} + l_r C_{y,r}}{I_{zz} v_x} & -\frac{C_{y,f} l_f^2 + C_{y,r} l_r^2}{I_{zz} v_x} \end{bmatrix} \begin{bmatrix} v_y \\ \dot{\psi}\end{bmatrix} + \begin{bmatrix} 0 & \frac{C_{y,f}}{m} \\ \frac{1}{I_{zz}} & \frac{l_f C_{y,f}}{I_{zz}} \end{bmatrix} \begin{bmatrix} M_z \\ \delta \end{bmatrix} \tag{6}$$

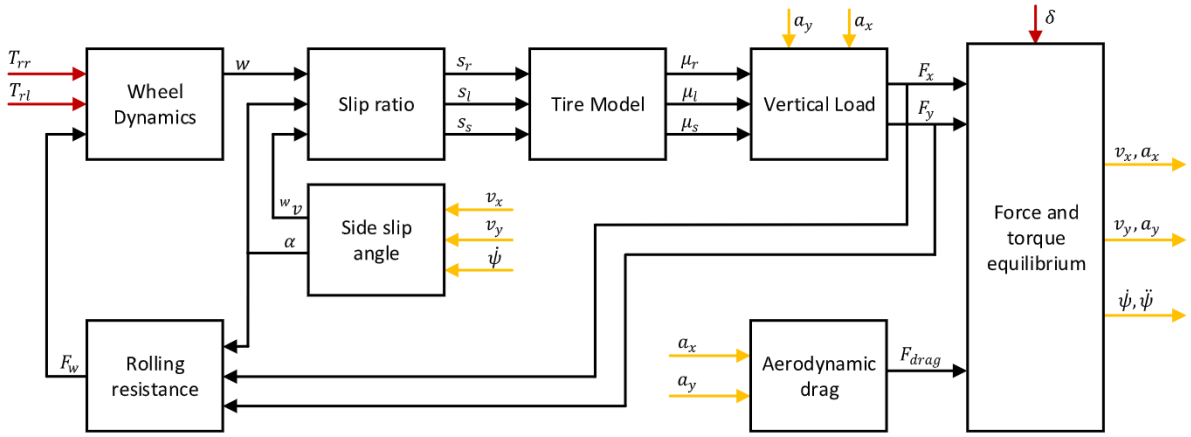

Fig. 1. Non-linear model diagram used by the FST team to simulate a Formula Student vehicle.

Table 2
FST06e specifications.

Term		Val	Units	Term		Val	Units
Mass	m	356	[kg]	Half track	t_r	0.65	[m]
Inertia moment	I_{zz}	120	[kg m^2]	Wheel radius	R_w	0.265	[m]
Front wheelbase	l_f	0.873	[m]	Front stiffness	$C_{y,f}$	15 714	[N/rad]
Rear wheelbase	l_r	0.717	[m]	Rear stiffness	$C_{y,r}$	21 429	[N/rad]

Table 3
Validation test results with differences between the model and the real data.

	Radius [m]	Vel. [m/s]	Steer [deg]	Yaw rate [deg/s]			Lateral velocity [m/s^2]		
				Real	Model	Diff	Real	Model	Diff
Test1	5.6	7.0	110	72.3	70.8	1.5	8.7	8.2	0.5
Test2	5.6	8.5	100	72.0	69.0	3.0	9.7	8.8	0.9
Test3	9.0	9.3	71	59.6	60.2	−0.6	8.9	8.0	0.9

2.3. Model validation

In order to validate the lateral dynamics, a series of skidpads (constant radius turns) were performed. The skidpad is defined by ISO 4138 [16], where the trajectory should have a minimum radius of 30 m. Due to the available tracks, the radius had to be decreased. Three tests were performed, two with a radius of 5.6 m and the third with 9 m. Note that a skid pad in a Formula Student competition has a radius of 8.75 m.

During the tests, six main variables were logged for validation purposes: (i) three inputs needed for the model i.e. the steering angle, torque and the global velocity of the vehicle; (ii) three outputs i.e. longitudinal acceleration, lateral acceleration, and yaw rate. The parameters of the tests, the average values during the turns, and differences to the non-linear model are presented in Table 3. In Fig. 2 it is possible to see the comparisons along time between the real data from the car and the models for the yaw rate and lateral velocity.

From Table 3 and Fig. 2, it is possible to see that the simulation model is close enough to the real data to be used in the controller testing.

To solve the same problem in another 4-wheel vehicle, it is sufficient to change the relevant specifications and to tune the controller parameters accordingly, maintaining the control architecture whereby disclosed.

3. Control system design

In this section, the design of the controller is proposed. First the calculations needed to achieve a reference value for the yaw rate are presented, followed by the design of a PID controller, and finalized with the design of a LQR controller.

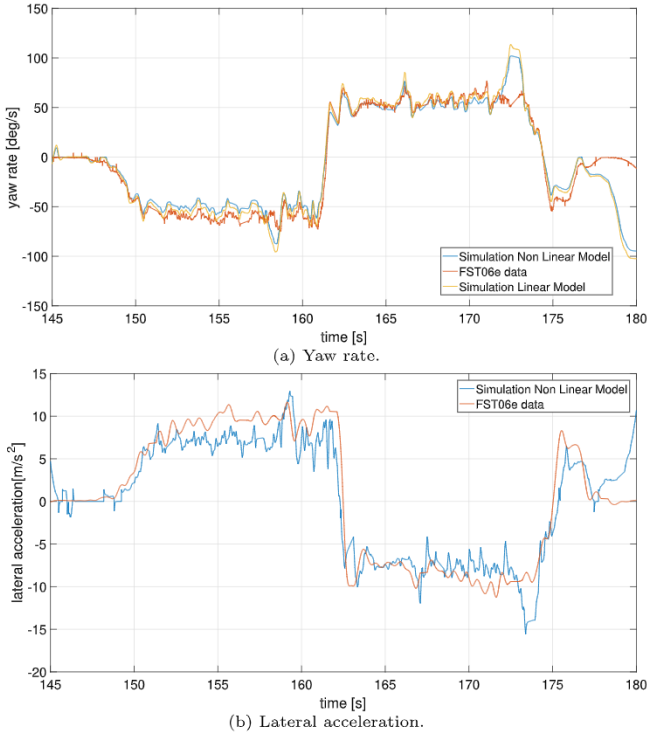

(a) Yaw rate.

(b) Lateral acceleration.

Fig. 2. Comparison between the validation results and the model.

3.1. Reference value

For this application, the yaw rate is chosen as the variable to be controlled, since for a constant radius turn a higher yaw rate represents a higher linear velocity and, therefore, a small lap time. However, this value is limited by the vehicle characteristics. Several authors propose the use of the steering angle and the velocity to compute this reference, and in all cases, it is assumed a steady state condition of the vehicle [13].

First, it is introduced the stability factor K_u, given by Eq. (7). If $K_u < 0$, the car is said to have an over-steer behavior. If $K_u > 0$, it is said to have an under-steer. If $K_u = 0$, the car is said to have neutral-steer. A neutral-steer vehicle has the minimal radius of turn possible. However, it is close to the instability (over-steer).

Table 4
Proportional and integral gains for several longitudinal velocity set-points.

v_x (m/s)	7	10	13	16	19	22
P gain	296.3	392.2	421.7	479.9	396.2	404.8
I gain	12 716.7	12 492.5	12 040.0	11 536.1	11 058.5	13 650

Therefore, the cars are projected to be close to the neutral-steer, but still have under-steer.

$$K_u = \frac{l_r m}{(l_f + l_r)^2 C_{y,f}} - \frac{l_f m}{(l_f + l_r)^2 C_{y,r}} \tag{7}$$

Through the definition of the curvature response [12] and the angular velocity expression, it is possible to write the desired yaw rate equation as (8), dependent of the longitudinal velocity and the steering angle. The stability factor can be used as an adjustment coefficient for tuning the response of the vehicle.

$$\dot{\psi}_{des} = \frac{v_x}{(l_f + l_r) + K_u (l_f + l_r) v_x^2} \delta \tag{8}$$

The maximum yaw rate is not infinite and is limited by several factors, like the road condition, the computing time of the controller and the entry velocity. In order to limit this value, Eq. (9), which uses as the limiting factor the tire-road coefficient, is introduced.

$$v_{cg} \dot{\psi} + a_x \beta + \frac{v_{cg} \dot{\beta}}{\sqrt{1 + \tan \beta^2}} \leq \mu g \tag{9}$$

This equation considers a small sideslip angle, and can be shortened to (10), where σ is an adjust coefficient for different road conditions. The yaw rate reference is then the absolute minimum value between the desired ($\dot{\psi}_{des}$) and the maximum ($\dot{\psi}_{max}$), as expressed by (11).

$$\dot{\psi}_{max} = \sigma \frac{\mu g}{v_{cg}} \tag{10}$$

$$\dot{\psi}_{ref} = \begin{cases} \dot{\psi}_{des}, & |\dot{\psi}_{des}| \leq |\dot{\psi}_{max}| \\ \pm \dot{\psi}_{max}, & otherwise \end{cases} \tag{11}$$

3.2. PI controller

As already stated, and shown in Eq. (3), the input used to control the yaw rate of the vehicle is a torque induced at the center of gravity (12). This is generated by a difference on the force produced by the rear wheels (driven wheels).

$$M_z = \left(F_x^{RR} - F_x^{RL}\right) t_f \tag{12}$$

For Eq. (12), it is assumed that all the force generated by the motor is applied on the vehicle and no slip occurs. Between the motor and the wheel exists a fixed gear ratio $G_r = 4.4$. For the proposed controller, the variation of torque ΔT applied to each motor is used, that can be easily written as (13). This equation is introduced in (6), for the final model used in the controller.

$$\Delta T = \frac{R_w}{2 G_r t_f} M_z = \frac{0.265}{2 \times 4.4 \times 0.65} M_z = 0.05 M_z \tag{13}$$

Since (6) is dependent of the longitudinal velocity, the PID controller must also change with v_x. Taking this into account, the gains were adjusted for different velocities, and a lookup table is implemented to change these gains with the current velocity. The PI controller specifications are: (i) overshoot below 10%; (ii) settling time of less than 0.2 s. The evolution of the coefficients can be seen in Table 4. Also in Fig. 3, it is possible to see the evolution of the frequency response for different low velocities.

3.3. LQR controller

A PI controller is simple, but has some limitations associated with that simplicity, namely the performance one of the most relevant. To improve this, a LQR (Linear Quadratic Regulator) is proposed. This one is a more robust controller to unpredicted changes in the platform, like an inaccurate tire-road coefficient, or an over optimistic yaw rate reference, that can bring the vehicle to an unstable condition.

The LQR controller is based on the same linear model as presented before (6). Additionally, besides the yaw rate, it also uses an observation of the lateral velocity. This one is given by (14), a geometric calculation that results in a noisy signal and has some error associated. Since the case study (skid pad) is a controlled environment, that is, the global velocity and the radius are constant, this approximation is valid. In a future application, some other observation method should be used, like a GPS, A-GPS, Differential GPS, a kinematic GPS, an Optical Flow [17], or an estimation algorithm like [18].

$$v_y = \sqrt{v_{CG}^2 + v_x^2}, \quad where \quad v_x = \sqrt{a_x / R} \tag{14}$$

For the model used (6), it is necessary to introduce an integral action to remove the steady-state error of the yaw rate. The model for the LQR can then be written as (15), where the input is the torque variation seen previously.

$$\begin{bmatrix} \dot{v}_y \\ \ddot{\psi} \\ \dot{\xi} \end{bmatrix} = \begin{bmatrix} -\frac{C_{y,f} + C_{y,r}}{m v_x} & \frac{-l_f C_{y,f} + l_r C_{y,r}}{m v_x} - v_x & 0 \\ \frac{-l_f C_{y,f} + l_r C_{y,r}}{I_{zz} v_x} & -\frac{C_{y,f} l_f^2 + C_{y,r} l_r^2}{I_{zz} v_x} & 0 \\ 0 & -1 & 0 \end{bmatrix} \begin{bmatrix} v_y \\ \dot{\psi} \\ \xi \end{bmatrix} + \begin{bmatrix} 0 \\ \frac{1}{0.05 I_{zz}} \\ 0 \end{bmatrix} \Delta T \tag{15}$$

For the gain computation, the weights used were $Q = diag\left(1, 1, 10^6\right)$ and $R = 10^{-6}$. This is also a time varying controller due to the longitudinal velocity. To overcome this, the same method, as reported in the previous section, is implemented. Several gains are computed offline for different velocities, and a lookup table is used during the actuation of the controller. In Fig. 4, the evolution of the gains for different increasing velocities are plotted.

4. Implementation

To analyze the performance of the proposed controllers, an implementation was made in a Formula Student prototype. The vehicle used for the test is the FST06e already presented before. The test is a series of skid pads with a 5 m radius. In this section, are detailed the acquisition system used on the vehicle, and the modifications required to the controllers. Finally, the results are compared, with and without controllers.

4.1. Test platform

This vehicle is equipped with a gyroscope, a steering encoder, a Global Positioning System (GPS) and four wheel encodes (one per wheel). Is propelled by two 50 kW independent electric motors, one per each rear wheel, that accept a torque setpoint, and can return the actual torque applied by the motor. For the proposed algorithm, the yaw rate is provided by the gyroscope, and the longitudinal velocity is a combination of the GPS velocity and the projected velocity of each wheel. In the vehicle, all these sensor readings are available in a single CAN-Bus line. The discrete

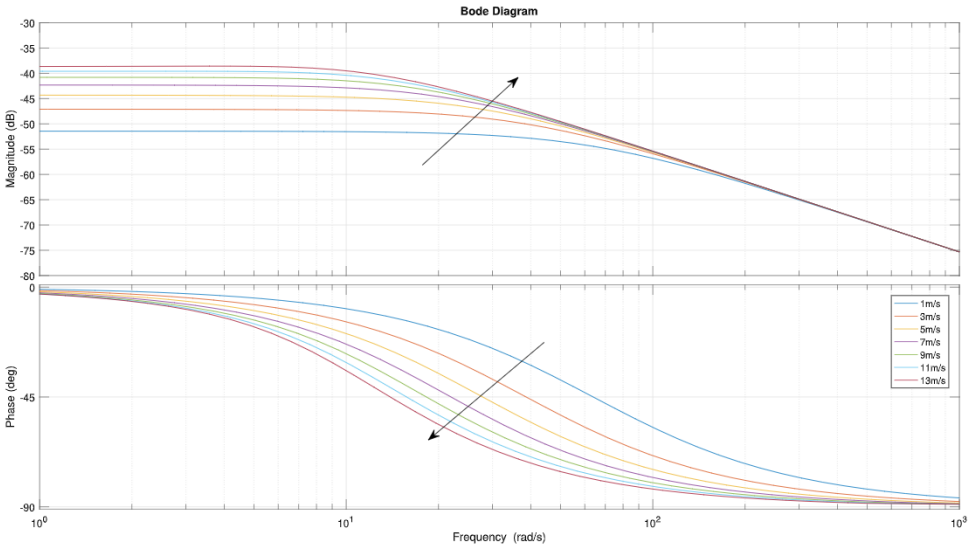

Fig. 3. Frequency response evolution of the PI controller for different longitudinal velocities.

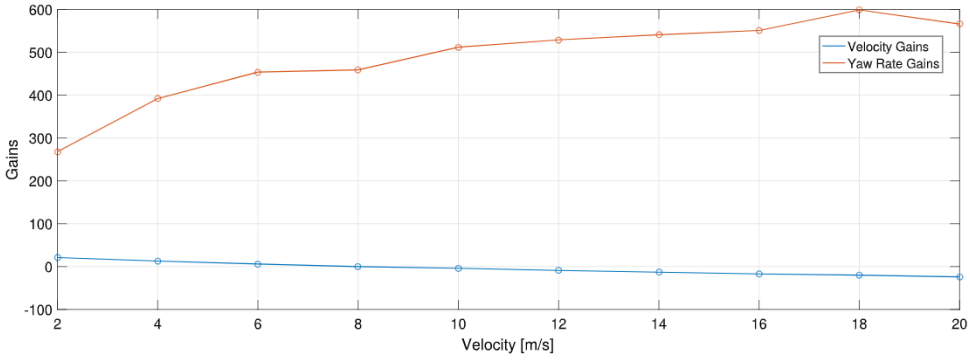

Fig. 4. LQR gain evolution for different longitudinal velocity set-points.

frequency used for the controllers implementation is 50 Hz. This value was set based on a compromise between the acquisition frequency of the sensors, the computational power available, and on a frequency analysis to the controllers.

4.2. Discrete controllers

The discrete PI controller had the same tuning process as the continuous version. The major modification is the implementation of an anti-windup mechanism. This is required due to the limitation of the torque input at the motors to a maximum of 107 N m and a minimum of 0 N m, which means no negative torque can be applied, for safety reasons.

For the LQR controller, the system (15) is first discretized using property (16), where index c represents continuous matrices, index d discrete matrices, T is the sampling time, and I the identity matrix, i.e. the step invariant method.

$$\begin{bmatrix} A_d & B_d \\ 0 & I \end{bmatrix} = \exp\left(\begin{bmatrix} A_c & B_c \\ 0 & 0 \end{bmatrix} T\right) \tag{16}$$

Before the controllers were implemented in the vehicle, a simulation with hardware in the loop was performed to guarantee the stability and performance of the system with discrete noise added from a micro-controller.

4.3. Results

The first test was made without the controllers, to be used as a reference without torque vectoring. In Fig. 5a it is presented the test results with the current yaw rate, the reference yaw rate to be used by a controller and the velocity, in yellow on the picture. The driver made five turns to each side with around five seconds per turn. These are easily identified by the almost constant yaw rate. From Fig. 5a, it is possible to see a difference of about 10 deg/s between the reference and the real value, which can be translated in gain from the controller. The second test is with the PI controller implemented. The results can be seen in Fig. 5b, where in this case the real yaw rate follows the reference with a very small difference.

In Fig. 6, it is presented the inputs of each motor compared with what would be a perfect turn in a simulation. In blue and orange are depicted the torque of the real vehicle, where it is clear the action of the controller during the turn. To note that the reference is dependent on the steering angle, and any minor correction made by the driver results in the oscillations seen in the orange signal. To note that in the real vehicle the minimum torque available is 0 N m.

In Table 5 it is presented the mean results with and without the torque vectoring controller, and for the same radius of turn and almost the same velocity. The lap time has been reduced in 7.6%. Additionally, the clearest evidence of the actuation of a torque vectoring controller is the G-G diagram presented in Fig. 7,

Table 5
Mean values for the comparison with and without torque vectoring on the FST06e.

	Yaw rate [deg/s]	Velocity [m/s]	Lap time [s]
Without torque vectoring	70	8.4	4.97
With torque vectoring	74	8.8	4.59

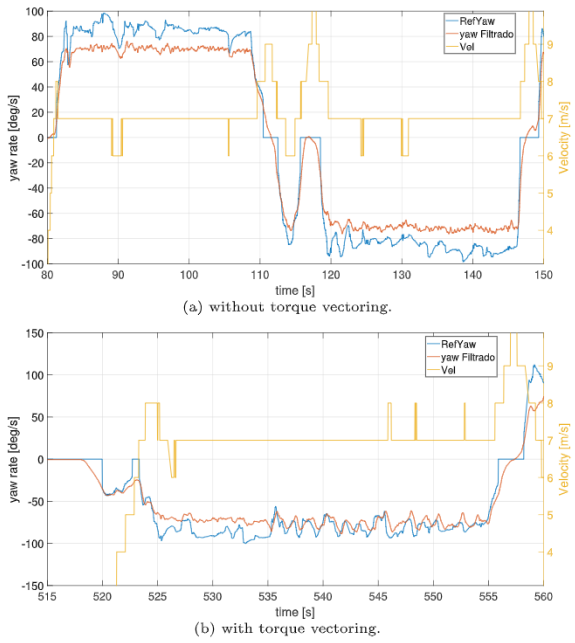

Fig. 5. Desired yaw rate (blue) and real yaw rate (orange). (For interpretation of the references to color in this figure legend, the reader is referred to the web version of this article.)

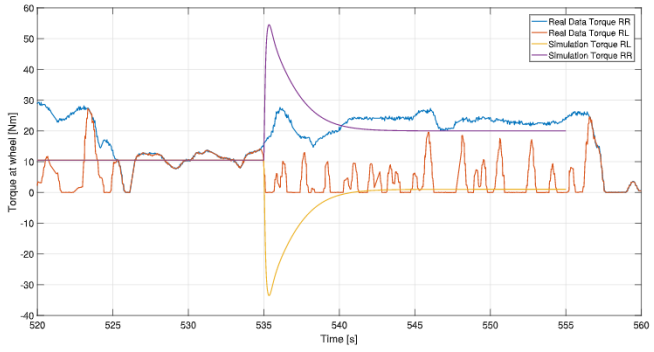

Fig. 6. Comparison between the real torque actuation signals (blue RR, orange RL) and the simulated (yellow RL and purple RR). (For interpretation of the references to color in this figure legend, the reader is referred to the web version of this article.)

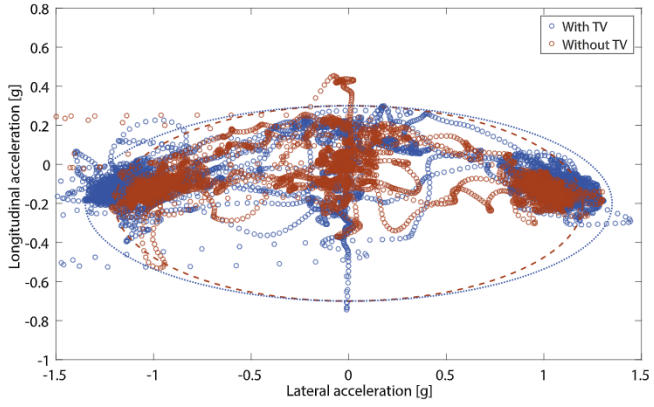

Fig. 7. G-G Diagram of the FST06e with and without torque vectoring.

where it is clear that the car for the same conditions can generate more lateral acceleration. Unfortunately, due to problems with the FST06e, it was impossible to log the data from the LQR, but the behavior presented in the track and the feedback from the driver are very encouraging.

5. Conclusion

A non-linear model was presented for a Formula Student vehicle with the required modifications for a torque vectoring implementation, as well as a linearized version. Both models were validated with real data from a Formula Student vehicle, showing very close results. The non-linear model was used in simulation to test the proposed controllers. A methodology for computing a reference, dependent of the steering angle, for the controllers is presented along with a tuning procedure. Two control strategies are proposed, a PI controller and a LQR controller. Both use the concept of removing torque from one driven wheel to the other, with the objective of generating an additional torque to increase the yaw rate of the vehicle. The PI controller uses only the yaw rate, is simpler to implement, and is more intuitive. The LQR uses also the lateral velocity to make the controller more robust.

Both controllers were discretized and implemented on a microcontroller, first in a bench test, to guarantee the stability of the code and algorithm, and later in the FST06e for a real track test. The data from the PI controller showed very promising results with a 7.6% time reduction in a 5 s turn for the same conditions without a controller, and a clear gain in the lateral acceleration. Due to log problems with the vehicle, the data from the LQR was not recorded, but the on-track performance and driver feedback proved to be quite promising.

Acknowledgments

This work was supported by FCT, Portugal, through IDMEC, under LAETA, project UID/EMS/50022/2013. The authors also thank the prompt and fruitful cooperation with the IST Formula Student team, FST Lisboa.

References

[1] J. Ghosh, A. Tonoli, N. Amati, A torque vectoring strategy for improving the performance of a rear wheel drive electric vehicle, in: 2015 IEEE Vehicle Power and Propulsion Conference (VPPC), 2015, pp. 1–6, http://dx.doi.org/10.1109/VPPC.2015.7352887.

[2] G. Kaiser, Q. Liu, C. Hoffmann, M. Korte, H. Werner, Torque vectoring for an electric vehicle using an lpv drive controller and a torque and slip limiter, in: 2012 IEEE 51st IEEE Conference on Decision and Control (CDC), 2012, pp. 5016–5021, http://dx.doi.org/10.1109/CDC.2012.6426553.

[3] G. Kaiser, F. Holzmann, B. Chretien, M. Korte, H. Werner, Torque vectoring with a feedback and feed forward controller - applied to a through the road hybrid electric vehicle, in: 2011 IEEE Intelligent Vehicles Symposium (IV), 2011, pp. 448–453, http://dx.doi.org/10.1109/IVS.2011.5940459.

[4] L.D. Novellis, A. Sorniotti, P. Gruber, A. Pennycott, Comparison of feedback control techniques for torque-vectoring control of fully electric vehicles, IEEE Trans. Veh. Technol. 63 (8) (2014) 3612–3623, http://dx.doi.org/10.1109/TVT.2014.2305475.

[5] D. Rubin, S. Arogeti, Vehicle yaw stability control using rear active differential via Sliding mode control methods, in: 21st Mediterranean Conference on Control and Automation, 2013, pp. 317–322, http://dx.doi.org/10.1109/MED.2013.6608740.

[6] A. Stoop, Design and Implementation of Torque Vectoring for the Forze Racing Car (Master's thesis), Delft Center for Systems and Control, 2014.

[7] S. Anwar, Yaw stability control of an automotive vehicle via generalized predictive algorithm, in: Proceedings of the 2005, American Control Conference, 2005., 2005, pp. 435–440, http://dx.doi.org/10.1109/ACC.2005.1469974.

[8] S.D. Cairano, H.E. Tseng, D. Bernardini, A. Bemporad, Vehicle yaw stability control by coordinated active front steering and differential braking in the tire sideslip angles domain, IEEE Trans. Control Syst. Technol. 21 (4) (2013) 1236–1248, http://dx.doi.org/10.1109/TCST.2012.2198886.

[9] C. Zhao, W. Xiang, P. Richardson, Vehicle lateral control and yaw stability control through differential braking, in: 2006 IEEE International Symposium on Industrial Electronics, Vol. 1, 2006, pp. 384–389, http://dx.doi.org/10.1109/ISIE.2006.295624.

[10] D. Schramm, M. Hiller, R. Bardini, Vehicle Dynamics: Modelling and Simulation, first ed., Springer, ISBN: 978-3-540-36045-2, 2014.

[11] D.M. Bevly, J. Ryu, J.C. Gerdes, Integrating ins sensors with gps measurements for continuous estimation of vehicle sideslip, roll, and tire cornering stiffness, IEEE Trans. Intell. Transp. Syst. 7 (4) (2006) 483–493, http://dx.doi.org/10.1109/TITS.2006.883110.
[12] R.N. Jazar, Vehicle Dynamics: Theory and Applications, second ed., Springer, ISBN: 978-1461485445, 2014.
[13] R. Rajamani, Vehicle Dynamics and Control, Mechanical Engineering Series, first ed., Springer, ISBN: 978-0387263960, 2005.
[14] U. Kiencke, L. Nielsen, Automotive Control Systems for Engine, Driveline, and Vehicle, second ed., Springer, ISBN: 978-3540231394, 2005.
[15] M. Abe, Vehicle Handling Dynamics: Theory and Application, first ed., Butterworth-Heinemann, ISBN: 978-1856177498, 2009.
[16] Passengers Cars - Steady-state Circular Driving Behaviour - Open-loop Test Methods ISO 4138:2004, fourth ed., 2012.
[17] M. Doumiati, A. Victorino, A. Charara, D. Lechner, A method to estimate the lateral tire force and the sideslip angle of a vehicle: Experimental validation, in: Proceedings of the 2010 American Control Conference, 2010, pp. 6936–6942, http://dx.doi.org/10.1109/ACC.2010.5531319.
[18] A. Antunes, C. Cardeira, P. Oliveira, Application of sideslip estimation architecture to a formula student prototype, in: A. Ollero, A. Sanfeliu, L. Montano, N. Lau, C. Cardeira (Eds.), ROBOT 2017: Third Iberian Robotics Conference. ROBOT 2017. Advances in Intelligent Systems and Computing, Vol. 694, Springer, Cham, 2018, pp. 409–421, http://dx.doi.org/10.1007/978-3-319-70836-2_34.

João Antunes graduated from Instituto Superior Técnico (IST), Lisbon, Portugal in 2017. He completed his master's degree in mechanical engineering with a thesis on Development of a Torque Vectoring System for a Rear Wheel Driven Electric Vehicle. He was a member of the formula student team. His research interests include automobiles and control methods.

André Antunes is a recently graduated student from Instituto Superior Técnico (IST), Lisbon, Portugal. He completed his master's degree in mechanical engineering with a thesis on Sideslip Estimation of Formula Student Prototype. He was a member of the formula student team. He is currently working at Tekever. His research interests include automobiles and estimation methods.

Pedro Outeiro is a recently graduated student from Instituto Superior Técnico (IST), Lisbon, Portugal. He completed his master's degree in mechanical engineering with a thesis on Control and Estimation Methods for Unknown Load Transportation with Quadrotors. He received three diplomas for academic excellence and one for academic merit during his studies.

He is aiming to further his studies by enrolling into a PhD program, allowing him also to continue the work he started with his master's thesis.

Carlos B. Cardeira was born in Quinjenje, Angola, and received the engineering and master of science degrees in 1986 and 1991, in electrical engineering from Instituto Superior Técnico in Lisbon–Portugal. In 1994 he received the PhD in electrical engineering and computer science from the Institut National Polytechnique de Lorraine in Nancy–France. He is a member of the Center of Intelligent Systems of the IDMEC research laboratory and teaches at Instituto Superior Técnico in Lisbon courses in Mechatronics Systems, Industrial Automation and Informatics areas. He made several post-docs and sabbatical leaves, namely in IRIT and LAAS in Toulouse–France, CERN in Geneva–Switzerland and Schneider-Electric in Seligenstadt–Germany.

Paulo Oliveira (Hab 16 PhD'02 MSc'91) received the "Licenciatura," M.S., and Ph.D. degrees in Electrical and Computer Engineering, and the Habilitation in Mechanical Engineering from Instituto Superior Técnico (IST), Lisbon, Portugal, in 1991, 2002, and 2016, respectively. He is an Associate Professor in the Department of Mechanical Engineering of IST and Senior Researcher in the Associated Laboratory for Energy, Transports, and Aeronautics. His research interests are in the area of autonomous robotic vehicles with a focus on the fields of estimation, sensor fusion, navigation, positioning, and mechatronics. He is author or coauthor of more than 65 journal papers and 175 conference communications. He participated in more than 30 European and Portuguese research projects, over the last 30 years.